Eur. Phys. J. C 27, 577–585 (2003)
Digital Object Identifier (DOI) 10.1140/epjc/s2003-01137-1

THE EUROPEAN PHYSICAL JOURNAL C

# Lepton flavor-changing scalar interactions and $g-2$ of the muon

Y.-F. Zhou[1,a], Y.-L. Wu[2,b]

[1] Ludwig-Maximilians-Universität München, Sektion Physik, Theresienstraße 37, 80333 München, Germany
[2] Institute of Theoretical Physics, Chinese Academy of Science, Beijing 100080, P.R. China

Received: 5 September 2002 / Revised version: 11 January 2003 /
Published online: 26 February 2003 – 

**Abstract.** A systematic investigation on the muon's anomalous magnetic moment and a related lepton flavor-violating process such as $\mu \to e\gamma$, $\tau \to e\gamma$ and $\tau \to \mu\gamma$ is made at the two-loop level in the models with flavor-changing scalar interactions. The two-loop diagrams with double scalar exchanges are studied and their contributions are found to be compatible with the ones from the Barr–Zee diagram. By comparing with the latest data, the allowed ranges for the relevant Yukawa couplings $Y_{ij}$ in the lepton sector are obtained. The results show the hierarchical structure $Y_{\mu e,\tau e} \ll Y_{\mu\tau} \simeq Y_{\mu\mu}$ in the physical basis if $\Delta a_\mu$ is found to be $> 50 \times 10^{-11}$. It deviates from the widely used ansatz in which the off-diagonal elements are proportional to the square root of the products of the related fermion masses. An alternative Yukawa coupling matrix in the lepton sector is suggested to understand the current data. With such a reasonable Yukawa coupling ansatz, the decay rate of $\tau \to \mu\gamma$ is found to be near the current experiment upper bound.

## 1 Introduction

Recently, the Muon $g-2$ Collaboration at BNL reported their improved result on the measurement of the muon's anomalous magnetic moment $(g-2)$ [1]. Combining with the early measurements in CERN and BNL, the new average value of the muon's $g-2$ is as follows:

$$a_\mu^{\rm exp} = (116592030 \pm 80) \times 10^{-11}. \qquad (1)$$

This result confirmed the earlier measurement [2] with a much higher precision. With this new result the difference between experiment and the standard model (SM) prediction is enlarged again. The most recent analyses by different groups resulted in

$$\Delta a_\mu \equiv a_\mu^{\rm exp} - a_\mu^{\rm SM} = \begin{cases} (303.3 \pm 106.9) \times 10^{-11} & [3], \\ (297.0 \pm 107.2) \times 10^{-11}({\rm ex}) & [4], \\ (357.2 \pm 106.4) \times 10^{-11}({\rm in}) & [4]. \end{cases} \qquad (2)$$

As the large $g-2$ of the muon may imply the existence of new physics beyond the SM, in recent years a large amount of work has been done in checking the new physics contributions to $g-2$ of the muon by using model dependent [5,6] and independent approaches [7].

In this work, we would like to focus on a general discussion of the models with lepton flavor-changing scalar interactions where the new physics contributions mainly arise from additional Yukawa couplings. Such models may be considered as a simple extension of the standard model (SM) with more than one Higgs doublet $\phi_i$ $(i > 1)$ but without imposing any discrete symmetry, for example, the extension of SM with two Higgs doublets (S2HDM) [8] as motivated by spontaneous $CP$ violation [9,10].

The general form of the Yukawa interaction reads

$$\mathcal{L}_{\rm Y} = \bar{\psi}_{\rm L}^i Y_{ij}^a \psi_{\rm R}^j \phi_a, \qquad (3)$$

where $Y_{ij}^a$ $(i,j = 1,2,3)$ are the Yukawa coupling matrices. The index $a = 1,2,\cdots$ labels the Higgs doublets. The behavior of the Yukawa interactions depends on the texture of the Yukawa coupling matrices. In general there are two kinds of ansatzes on the Yukawa coupling matrices in the mass eigenstates:

(1) Yukawa coupling matrices of the scalar interactions are diagonal due to some discrete global symmetry [11];
(2) the Yukawa coupling matrices contain non-zero off-diagonal elements which are naturally suppressed by the light quark masses [12,13].

In the following sections (Sects. 2 and 3) we discuss at the two-loop level the constraints on those Yukawa coupling matrix elements under the above two ansatzes, and we will mainly focus on the latter one. One kind of two-loop diagrams with double scalar exchanges is studied in detail and their contributions to $g-2$ of the muon are found to be compatible with the one from the Barr–Zee diagram. In Sect. 4, combined constraints from $g-2$ of the muon and several lepton flavor violating (LFV) processes

[a] e-mail: zhou@theorie.physik.uni-muenchen.de
[b] e-mail: ylwu@itp.ac.cn

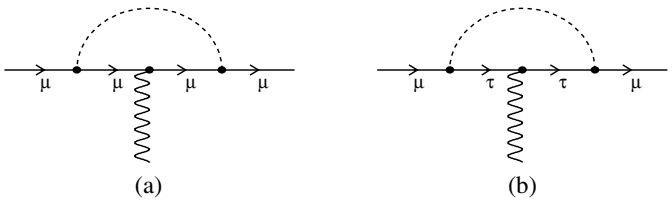


**Fig. 1a,b.** One-loop diagram contribution to $g-2$ of the muon. The dashed curves represent the scalar or pseudo-scalar propagator. **a** Flavor-conserving Yukawa interactions. **b** Flavor-changing Yukawa interactions in which $\mu$ changes into $\tau$ in the loop

are obtained. We note that unlike other experiments which often impose upper bounds of the parameters in the new physics models, the current data on $g-2$ of the muon may provide non-trivial lower bounds. It is found that the small lower bound of $\Delta a_\mu > 50\times10^{-11}$ will significantly modify the texture of the Yukawa coupling matrix and make it deviate from the widely used ansatz in which the off-diagonal elements are proportional to the square root of the products of related fermion masses.

## 2 Muon $g-2$ from diagonal Yukawa couplings

The ansatz of zero off-diagonal matrix elements is often used to avoid the flavor-changing neutral current (FCNC) at tree level which was originally suggested from kaon physics, such as $K\to\mu^+\mu^-$ decay and $K^0$–$\overline{K}^0$ mixing. Such a texture structure of the Yukawa couplings can be obtained by imposing some kind of discrete symmetries [11]. The minimal SUSY standard model (MSSM) and the two-Higgs doublet model (2HDM) of type I and II can be catalogued into this type. In such models, the Yukawa interactions are flavor conserving and the couplings are proportional to the related fermion masses:

$$Y_{ii}=\frac{gm_i}{2m_W}\xi_i \quad\text{and}\quad Y_{ij}=0 \quad (i\neq j), \tag{4}$$

where $g$ is the weak coupling constant and $m_W$ is the mass of the $W$ boson. $\xi_i$ is the rescaled coupling constant. In the minimal SUSY model and the 2HDM of type II, $\xi_i=\tan\beta(\cot\beta)$ for down (up) type fermions.

The corresponding Feynman diagrams contributing to $g-2$ of the muon at one-loop level which is shown in Fig. 1a, these have recently been discussed and compared with the current data in [14–16].

As the muon lepton mass is small, i.e., $m_\mu\ll m_\phi$, where $m_\phi$ is the mass of the scalar ($\phi=h$) or pseudo-scalar ($\phi=A$), the one-loop contribution to $g-2$ of the muon can be written as [17]

$$\Delta a_\mu=\pm\frac{1}{8\pi^2}\frac{m_\mu^2}{m_\phi^2}\ln\left(\frac{m_\phi^2}{m_\mu^2}\right)Y_{ii}^2, \tag{5}$$

where the sign "+ (−)" is for scalar ($\phi=h$) (pseudo-scalar $\phi=A$) exchanges. It can be seen from the above equation

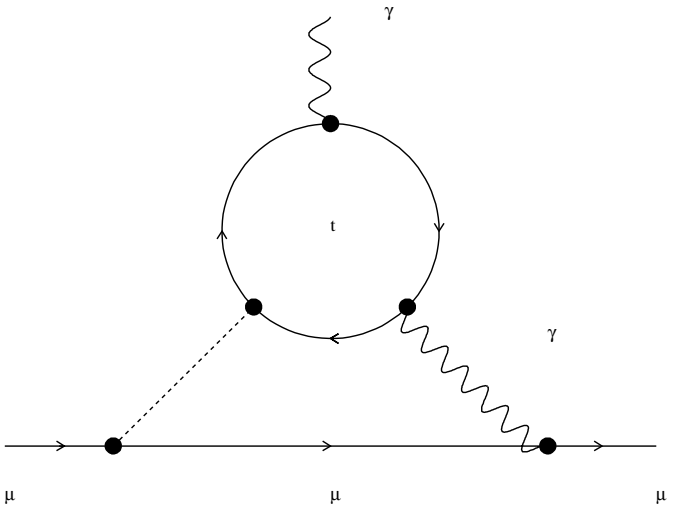


**Fig. 2.** Two-loop Barr–Zee diagram contribution to $g-2$ of the muon

that the one-loop scalar contribution is not large enough to explain the current data. Even for the large value of $\xi_\mu=\tan\beta\sim50$, one still needs a very light mass of the scalar: $M_h\sim5\,\mathrm{GeV}$, which does not seem to be favored by the LEP experiment. The situation will be even worse when both the scalar and pseudo-scalar are included, as their contributions have opposite signs.

The situation may be quite different if one goes to the two-loop level. This is because of the well known Barr–Zee mechanism [18] (see Fig. 2) in which the scalar or pseudo-scalar couples to a heavy fermion loop. As the Yukawa couplings are no longer suppressed by the light fermion mass, the two-loop contributions could be considerable. Taking the top quark loop as an example, the two-loop Barr–Zee diagram contribution to $g-2$ of the muon is given by

$$\Delta a_\mu^h=\frac{N_c q_t^2}{\pi^2}\frac{m_\mu m_t}{m_\phi^2}F\left(\frac{m_t^2}{m_\phi^2}\right)Y_{tt}Y_{\mu\mu}, \tag{6}$$

where $N_c=3$ and $q_t=2/3$ are the color number and the charge of the top quark, respectively. The integral function $F(z)$ has the following form [18]:

$$F(z)=\begin{cases}-\dfrac{1}{2}\displaystyle\int_0^1\mathrm{d}x\frac{1-2x(1-x)}{x(1-x)-z}\ln\frac{x(1-x)}{z}\\ \text{for scalar,}\\ \dfrac{1}{2}\displaystyle\int_0^1\mathrm{d}x\frac{1}{x(1-x)-z}\ln\frac{x(1-x)}{z}\\ \text{for pseudo-scalar.}\end{cases} \tag{7}$$

It is noticed that the contributions from the Barr–Zee diagram through scalar and pseudo-scalar exchanges have also different signs, negative for the scalar and positive for the pseudo-scalar, which is just opposite to the one-loop case. Thus there exists a cancellation between one- and two-loop diagram contributions. It was found in [19,20] that the pseudo-scalar exchanging Barr–Zee diagram can

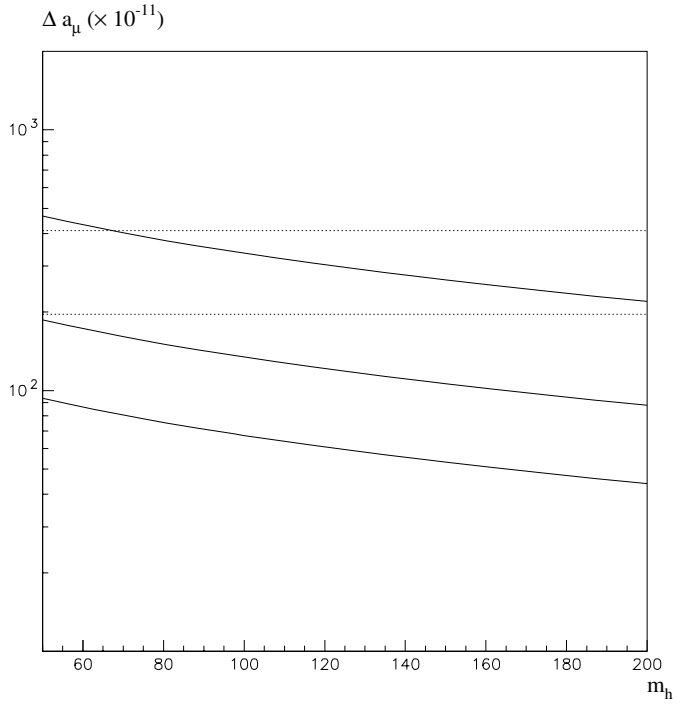


**Fig. 3.** Contribution to $g-2$ of the muon from the two-loop Barr–Zee diagrams. The three solid curves (from down to up) correspond to $Y_{\mu\mu}$ $(\xi_\mu) = 2\times10^{-2}$ (48.3), $4\times10^{-2}$ (97.6) and $1\times10^{-1}$ (273.9) respectively. The horizontal lines represent the $1\sigma$ allowed range from [3]

overwhelm its negative one-loop contributions and results in a positive contribution to $g-2$. For a sufficient large value of the coupling, $\xi_\mu = \tan\beta \sim 50$, its contribution can reach the $2\sigma$ experimental bound with $m_\phi \leq 70\,\mathrm{GeV}$. To avoid the cancellation between scalar and pseudo-scalar exchange, the mass of the scalar boson has to be pushed to be very heavy (typically greater than 500 GeV). In Fig. 3 the numerical calculation of the Barr–Zee diagram contribution to the $g-2$ of the muon is presented; it agrees with those results.

## 3 Muon $g-2$ from off-diagonal Yukawa couplings

When imposing the strict discrete symmetries to the Yukawa interaction, the off-diagonal elements of the Yukawa coupling matrix are all zero. This is the simplest way to prevent the theory from tree level FCNC. However, to meet the constraints from the data on $K^0$–$\overline{K}^0$ mixing and $K\to\mu^+\mu^-$ the off-diagonal elements do not necessarily have to be zero. An alternative way is to impose some approximate symmetries such as global family symmetry [8] on the Lagrangian. This results in the second ansatz of the Yukawa matrices in which small off-diagonal matrix elements are allowed, which leads to an enhancement for many flavor-changing processes. As the constraints from $K^0$–$\overline{K}^0$ mixing are strong, the corresponding off-diagonal matrix elements should be very small. However, up to now there are no such strong experimental constraints on the FCNC processes involving heavier flavors such as $c$ and $b$ quarks. The possibility of off-diagonal elements associated with the second and the third generation fermions are not excluded.

One of the widely used ansatzes of the Yukawa matrix based on the hierarchical fermion mass spectrum $m_{u,d} \ll m_{c,s} \ll m_{t,b}$ was proposed by Cheng and Sher [12,13]. In this ansatz, the off-diagonal matrix element has the following form:

$$Y_{ij} = \frac{g\sqrt{m_i m_j}}{2m_W}\xi_{ij}, \tag{8}$$

where the $\xi_{ij}$ are the rescaled Yukawa couplings which are roughly of the same order of magnitudes for all $i,j$. In this ansatz, the scalar or pseudo-scalar mediating the $d$–$s$ transition is strongly suppressed by the small factor $(m_d m_s)^{1/2}/(2m_W) \simeq 4\times10^{-4}$, which easily satisfies the constraints from $\Delta m_K, \epsilon_K$ and $\Gamma(K\to\mu^+\mu^-)$. As the couplings grow larger for heavier fermions, the tree level FCNC processes may give considerable contributions in $B^0$–$\bar{B}^0$ mixing, $\mu^+\mu^-\to tc,\mu\tau$ and several rare $B$ and $\tau$ decay modes [21–24].

Unlike the flavor-conserving one-loop diagrams, the flavor-changing one-loop diagrams (see Fig. 1b) with internal heavy fermions can give a large contribution to $g-2$ of the muon. The reason is that the loop integration yields an enhancement factor of $\sim m_i \ln(m_i^2/m_\phi^2)/(m_\mu \ln(m_\mu^2/m_\phi^2))$. For the internal $\tau$ loop, it is a factor of $\mathcal{O}(10)$. If one uses the scaled coupling $\xi_{\mu\tau}$ and takes $\xi_{\mu\tau} \simeq \xi_\mu$ as in the "Cheng–Sher" ansatz, the value of the enhancement factor can reach $\mathcal{O}(10^2)$. In the following discussion, for simplicity we only take one-loop diagram with an internal $\tau$ loop into consideration as it is dominant over other fermion loops in the case that the Yukawa couplings are of the same order of magnitudes.

The expression of the one-loop flavor-changing diagram contribution to the muon's $g-2$ is given by [25]

$$\Delta a_\mu = \pm\frac{1}{8\pi^2}\frac{m_\mu m_\tau}{m_\phi^2}\left(\ln\frac{m_\phi^2}{m_\tau^2} - \frac{3}{2}\right)Y_{\mu\tau}^2, \tag{9}$$

where the sign "+ (−)" is for scalar ($\phi = h$) (pseudo-scalar $\phi = A$) exchanges. For a detailed discussion of the one-loop flavor-changing diagram, we refer to [26,27].

As the two-loop contribution to $g-2$ of the muon is more considerable via the Barr–Zee mechanism in the flavor-conserving case, it is natural to go further by considering the same diagram with flavor-changing couplings. However, in the case of $g-2$ of the muon, as the initial and final states are all muons, it is easy to see that the Barr–Zee diagram with flavor-changing coupling cannot contribute. It can only appear in a flavor-changing process such as $\mu\to e\gamma$.

The non-trivial two-loop diagrams which give a non-negligible contribution to $g-2$ are those diagrams (as shown in Fig. 9) which have two internal scalars with both of them coupling to a heavy fermion loop.

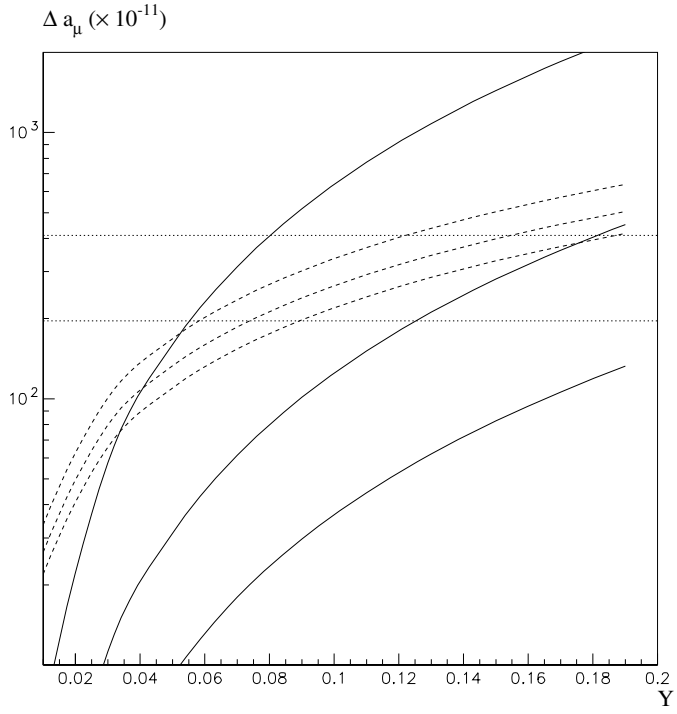


**Fig. 4.** Comparison between two-loop Barr–Zee pseudo-scalar and double pseudo-scalar exchanging diagram in the contribution to $g-2$ of the muon. The contribution to $g-2$ of the muon is plotted as a function of $Y = Y_{\mu\tau} = Y_{\mu\mu}$. The three solid curves (from up to down) correspond to the double scalar exchanging diagram contribution with scalar (pseudo-scalar) mass $m_A = 100, 150$ and $200\,\mathrm{GeV}$ respectively. The three dashed curves indicate the ones from two-loop Barr–Zee diagrams with pseudo-scalar exchange. The horizontal lines represent the $1\sigma$ allowed range from [3]

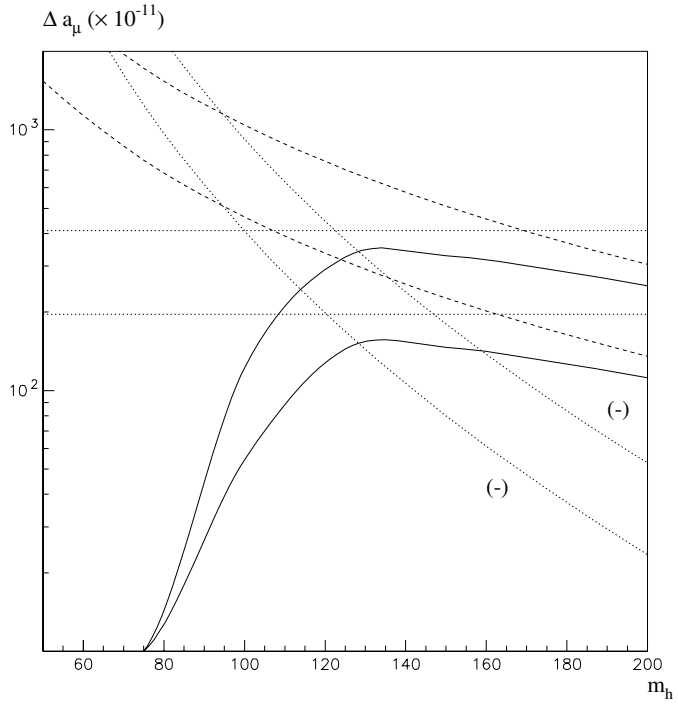


**Fig. 5.** Comparison between the one-loop and two-loop double scalar exchange diagrams in the contribution to $g-2$ of the muon. The contribution to $g-2$ of the muon is plotted as a function of the scalar mass. The two dashed curves represent the contribution at one loop with $Y_{\mu\tau}$ ($\xi_{\mu\tau}$) $= 0.12$ (70.6) (up) and 0.08 (47) (down) respectively. The two dotted curves correspond to the one from the two-loop double scalar diagram with the same couplings. (Note that their contributions are negative.) The solid curves are the total contributions to $g-2$ from both diagrams. The horizontal lines represent the $1\sigma$ allowed range from [3]

It is known that large Yukawa couplings between scalar and heavy fermions can compensate the loop suppressing factor $g^2/16\pi^2$ and make the Barr–Zee diagram sizable. The same mechanism also enhances the two-loop double scalar exchanging diagrams. Furthermore, in the flavor-changing case, the $\mu$ lepton can go into a heavier $\tau$ lepton in the lower loop, and this may provide an additional enhancement in the loop integration. Taking the internal $t$-quark loop as an example, the ratio between the contribution to $g-2$ of the muon from two-loop double scalar diagrams relative to the one from Barr–Zee type diagrams can be roughly estimated by the ratio between the couplings, which gives $\sim \xi_t \xi_{\mu\tau}^2 m_t m_\tau / (4\xi_\mu m_W^2 \sin^2\theta_{\mathrm{W}})$, where $\theta_{\mathrm{W}}$ is the Weinberg angle with the value $\sin^2\theta_{\mathrm{W}} \simeq 0.23$. For the typical values of $\xi_t = 1$ and $\xi_{\mu\tau} \simeq \xi_\mu = 30$ the ratio is of order 1. Thus this kind of two-loop double scalar exchanging diagram is compatible with the one of Barr–Zee type. In the large $m_t$ limit, the contribution to $g-2$ of the muon from the two-loop double scalar (pseudo-scalar) exchanging diagram has the following form:

$$\Delta a_\mu = \mp \frac{N_C m_\tau m_\mu m_t^2}{16\pi^4 m_\phi^4} \left( -\frac{5}{2} + \ln \frac{m_\phi^2}{m_\tau^2} \right) Y_{tt}^2 Y_{\mu\tau}^2. \quad (10)$$

The details of the two-loop calculations can be found in the appendix. Comparing with the one-loop flavor-changing diagram in the same way, one can see that the contribution from this diagram could be sizable.

For comparison, the contribution to $g-2$ of the muon from two-loop double pseudo-scalar exchanging diagrams and Barr–Zee diagrams with a pseudo-scalar are shown in Fig. 4.

To make the two kind of contributions comparable, we take $Y_{\mu\mu} = Y_{\mu\tau} \equiv Y$. It can be seen that the contribution from the former highly depends on the coupling $Y$ and the scalar mass. In the range $0.05 \leq Y \leq 0.15$, the contribution from the double scalar exchanging diagram is much larger than the one from the Barr–Zee diagram when $m_A$ is about $100 \sim 150\,\mathrm{GeV}$. It decreases with $m_A$ increasing and becomes quite small when $m_A \sim 200\,\mathrm{GeV}$.

In Fig. 5, the contribution to $g-2$ of the muon from two-loop double scalar exchanging diagrams is compared with the one from the corresponding flavor-changing one-loop diagrams.

Note that just like the case of the Barr–Zee diagram, the two-loop double scalar (pseudo-scalar) exchanging diagrams give negative (positive) contributions, which have

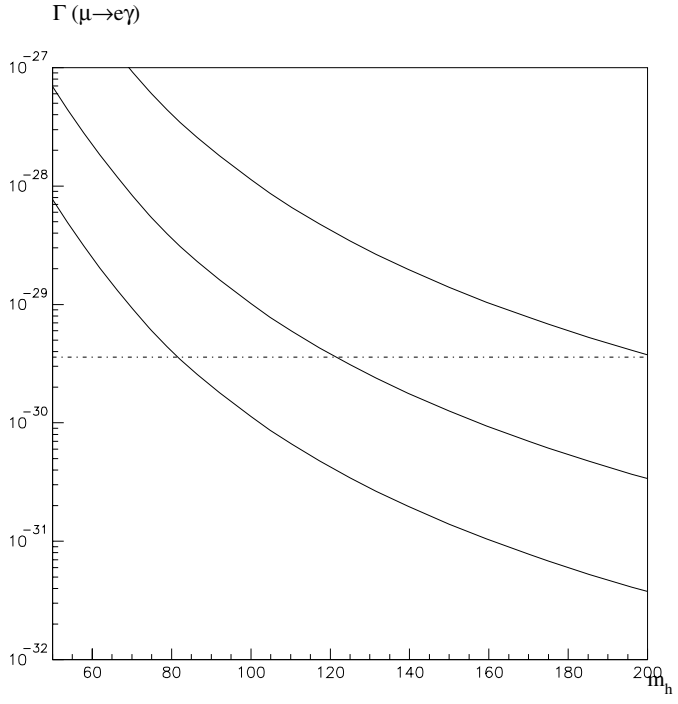


**Fig. 6.** The contribution to the decay $\mu \to e\gamma$ from the sum of one-loop and two-loop double scalar diagrams. The three solid curves (from down to up) correspond to $Y_{\tau e} = 1\times10^{-6}, 3\times10^{-6}$ and $1\times10^{-5}$ respectively. The coupling $Y_{\mu\tau}$ is taken to be 0.08. The horizontal line indicates the experimental upper bound of $\mu \to e\gamma$

signs opposite to the one from the one-loop scalar (pseudoscalar) exchanging diagram. The reason is that a closed fermion loop always contributes a minus sign. This results in a strong cancellation between one- and two-loop diagram contributions in the case of flavor-changing couplings with real Yukawa coupling constants. The allowed range of the scalar mass will be strongly constrained. Taking $Y_{\mu\tau} = 0.08$ ($\xi_{\mu\tau} \simeq 50$), $Y_{tt} = 0.67$ ($\xi_t \simeq 1$) and $\Delta a_\mu > 50 \times 10^{-11}$ as an example, the mass of the scalar $m_h$ lies in the narrow window of $\sim 100 \leq m_h \leq 200\,\mathrm{GeV}$.

## 4 Lepton flavor-violation processes and the texture of the Yukawa matrix

The flavor-changing Yukawa couplings will unavoidably lead to the enhancement of the decay rates of lepton flavor-violating processes. such as $\mu \to e\gamma$, $\tau \to \mu(e)\gamma$, $\mu \to e^-e^-e^+$ and $\tau \to e^-e^-e^+(\mu^-\mu^-\mu^+)$. The current experimental data, especially the data of $\mu \to e\gamma$ will impose the strongest constraints on the related Yukawa couplings. From the current data the upper bound of the decay $\mu \to e\gamma$ is $\Gamma(\mu \to e\gamma) \leq 3.6 \times 10^{-30}\,\mathrm{GeV}$ [28]. It constrains the coupling $Y_{e\tau(\mu)}$ to extremely small values.

In the models with flavor-changing scalar interactions, the leading contributions to $\mu \to e\gamma$ come from the one-loop flavor-changing diagram, the two-loop double scalar exchanging diagram and the two-loop flavor-changing Barr–Zee diagrams.

The effective vertex for the one-loop flavor-changing scalar interaction reads [29]

$$\Gamma_\mu^{\mathrm{one}} = \frac{1}{2(4\pi)^2}\frac{m_\tau}{m_\phi^2}\left(\ln\frac{m_\phi^2}{m_\tau^2} - \frac{3}{2}\right) Y_{\mu\tau}Y_{\tau e}\bar{\ell}\mathrm{i}\sigma_{\mu\nu}\ell q^\nu, \quad (11)$$

while the one for two-loop double scalar exchange is

$$\Gamma_\mu^{\mathrm{two}} = \frac{N_C m_\tau m_f^2}{32\pi^4 m_\phi^4}\left(\ln\frac{m_\phi^2}{m_\tau^2} - \frac{5}{2}\right) Y_{ff}^2 Y_{\mu\tau}^2 \bar{\ell}\mathrm{i}\sigma_{\mu\nu}\ell q^\nu. \quad (12)$$

In Fig. 6 the decay rates from the sum of the first two diagrams are presented as a function of the scalar mass. In the calculation we take the value of the coupling $Y_{tt} = 0.67$ (or $\xi_t \simeq 1$). The value of $Y_{\mu\tau}$ is taken to be 0.08 (or $\xi_{\mu\tau} \simeq 50$) which is the typical allowed value from the current data on $g-2$. It can be seen from the figure that the decay rates of $\mu \to e\gamma$ constrain the value of $Y_{\tau e}$ to no more than $10^{-6} \sim 10^{-5}$ for $100 \leq m_h \leq 200\,\mathrm{GeV}$.

Similarly, the value of the coupling $Y_{\mu e}$ is also constrained to be very small by the decay rate $\mu \to e\gamma$. The reason is that $Y_{\mu e}$ is associated with the flavor-changing Barr–Zee diagram in which a muon goes into a tau in the lower loop. If there is no accidental cancellation with other diagrams the upper bound of $Y_{\mu e}$ can be obtained by assuming that the flavor-changing Barr–Zee diagram is dominant. The decay rate of $\mu \to e\gamma$ from this diagram alone can be obtained from (6) and is given by

$$\Gamma^{\mathrm{BZ}}(\mu \to e\gamma) = 8\alpha m_\mu^5 \left|\frac{N_c q_t^2}{\pi^2}\frac{m_\mu m_t}{m_\phi^2}F\left(\frac{m_t^2}{m_\phi^2}\right) Y_{tt}Y_{\mu\mu}\right|^2 \quad (13)$$

The numerical result is represented in Fig. 7, which shows that the upper bound of $Y_{\mu e}$ is also of the order $10^{-6} \sim 10^{-5}$ for $100 \leq m_h \leq 200\,\mathrm{GeV}$.

With the above constraints on the values of the Yukawa couplings in the lepton sector, let us discuss the possible texture of the Yukawa coupling matrix. In the SM with one Higgs doublet, it is well known that by assuming the Yukawa matrix to be of the Fritzsch form [31,30] in the flavor basis, i.e.

$$Y \simeq \begin{pmatrix} 0 & \sqrt{m_1 m_2} & 0 \\ \sqrt{m_1 m_2} & 0 & \sqrt{m_2 m_3} \\ 0 & \sqrt{m_2 m_3} & m_3 \end{pmatrix}, \quad (14)$$

one can reproduce not only the correct quark masses in the mass eigenstates but also, to a good approximation, some of the mixing angles. In the models with multi-Higgs doublets, one can simply extend this Fritzsch parameterization to all the other Yukawa matrices including the leptons [12]. This results in the ansatz as in (8) with all $\xi_{ij}$ being of the same order of magnitude.

It is not difficult to see that such an ansatz may be challenged by the current experimental data in the lepton sector. This is because in order to explain the possible large $g-2$ of the muon, the off-diagonal elements connecting the second and third families should be enhanced,

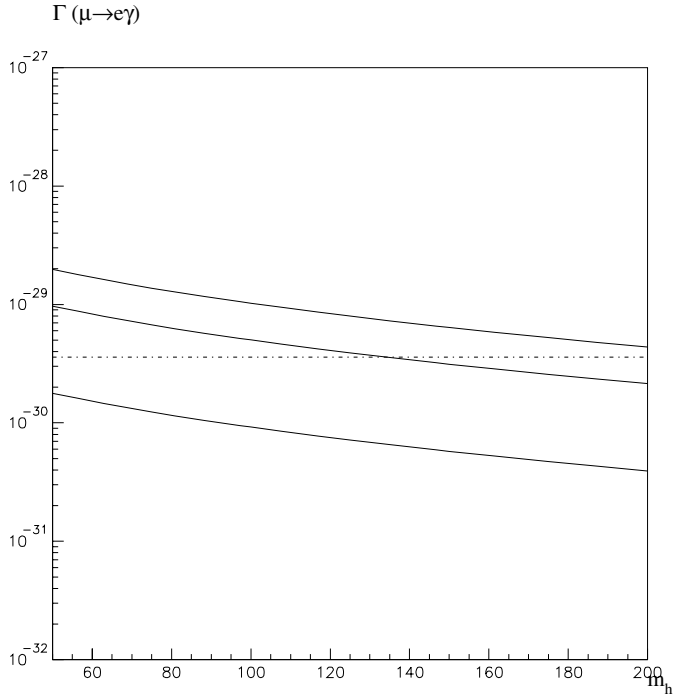


**Fig. 7.** Contribution to the decay $\mu \to e\gamma$ from the two-loop flavor-changing Barr–Zee diagrams. The three solid curves (from down to up) correspond to $Y_{\mu e} = 3\times10^{-6}, 7\times10^{-6}$ and $1\times10^{-5}$, respectively. The horizontal line indicates the experimental upper bound of $\mu \to e\gamma$

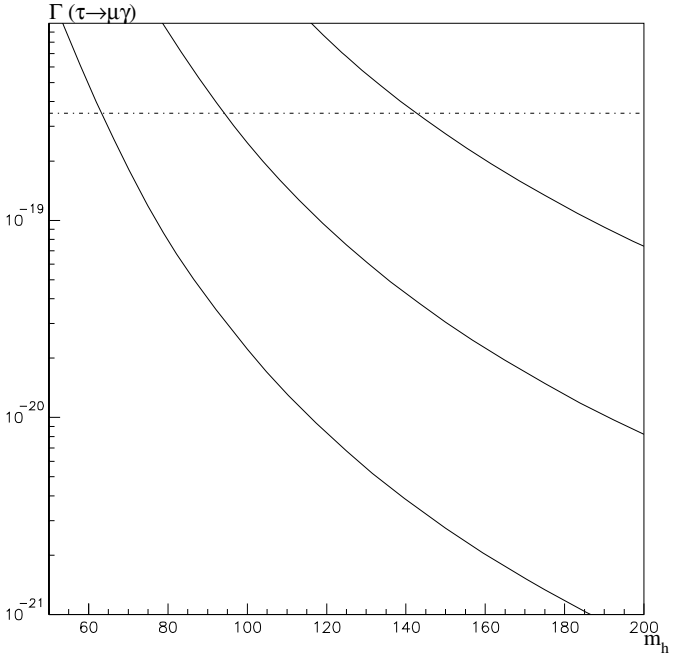


**Fig. 8.** Prediction of the decay rate $\tau \to \mu\gamma$ from the sum of one-loop and two-loop double scalar diagrams. The three solid curves (from down to up) correspond to $Y_{\tau\tau}$: 0.003, 0.01 and 0.03 respectively. The coupling $Y_{\mu\tau}$ is taken to be 0.08. The horizontal line indicates the experimental upper bound of $\tau \to \mu\gamma$

while to meet the constraints from $\mu \to e\gamma$, the ones connecting the first and second or the first and third families should be greatly suppressed.

Taking the values of $\Delta a_\mu > 50\times10^{-11}$, $m_h \sim 150\,\mathrm{GeV}$ and $m_A \gg m_h$ as an example, in the case of $g-2$ of the muon, if the flavor-conserving Barr–Zee diagram is playing a major role, the rescaled coupling $\xi_\mu$ should be as large as 50 (see Fig. 3). If one assumes that the flavor-changing coupling is responsible for the large $g-2$ of the muon, $\xi_{\mu\tau}$ ($Y_{\mu\tau}$) should be about 10 (0.02). On the other hand, due to the strong constraint from $\mu \to e\gamma$, for the flavor-changing contribution being the dominant case, $\xi_{\tau e}$ has to be less than 0.08 when $\xi_{\mu\tau}$ ($Y_{\mu\tau}$) is taken to have the typical value of 17.6 (0.03). In the case of a flavor-changing Barr–Zee diagram being dominant, the Yukawa coupling $\xi_{\mu e}$ has to be less than 0.24. Thus one finds that

$$\begin{aligned} \xi_\mu \sim \xi_{\mu\tau} &\simeq \mathcal{O}(10), \\ \xi_{\tau e} \sim \xi_{\mu e} &\simeq \mathcal{O}(10^{-1}), \end{aligned} \tag{15}$$

which clearly indicates that the rescaled couplings $\xi_{ij}$ are not of the same order of magnitude. In the case of a light pseudo-scalar mass $m_A \simeq 150\,\mathrm{GeV}$ and $m_h \gg m_A$ the results are similar.

From these considerations, it is suggested that the Yukawa matrices associated with the physical scalar bosons may take the following form in the mass eigenstate:

$$Y \simeq \lambda^2 \begin{pmatrix} \mathcal{O}(1) & \mathcal{O}(\lambda^n) & \mathcal{O}(\lambda^n) \\ \mathcal{O}(\lambda^n) & \mathcal{O}(1) & \mathcal{O}(1) \\ \mathcal{O}(\lambda^n) & \mathcal{O}(1) & \mathcal{O}(1) \end{pmatrix}, \tag{16}$$

where $\lambda \approx 0.22$ is roughly of the same order; $\lambda$ is the Wolfenstein parameter, and $n \simeq 2 \sim 3$. With such a parameterization, one is able to understand all the current experimental data concerning both $g-2$ of the muon and lepton flavor-changing processes.

If one takes the Yukawa matrix to be of the form in (16), the decay rate of $\tau \to \mu\gamma$ could be predicted. To a good approximation, the decay rate can be obtained by replacing $Y_{\mu\tau}Y_{\tau e}$ into $Y_{\tau\tau}Y_{\tau\mu}$ in (11) and (12).

Assuming $\tau$ lepton dominance in the loop, the contributions to $\tau \to \mu\gamma$ are shown in Fig. 8. The current upper bound on $\tau \to \mu\gamma$ is $3.5\times10^{-19}\,\mathrm{GeV}$ [28]. It is found that the predicted decay rate could reach the current experimental bound. A modest improvement in the precision of the present experiment for $\tau \to \mu\gamma$ may yield first evidence of lepton family number non-conservation.

In summary, we have studied the $g-2$ of the muon and several lepton flavor violation processes in the models with flavor-changing scalar interactions. The two-loop diagrams with double scalar exchanges have been investigated and their contribution to $g-2$ of the muon is found to be compatible with the one from the Barr–Zee diagram. The constraints on the Yukawa coupling constants have been obtained from the current data of $g-2$ of the muon and several lepton flavor-violation processes. The results have shown very strong constraints on the flavor-changing

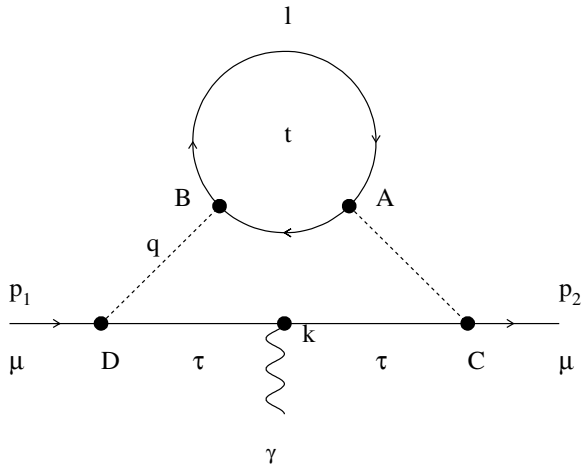


**Fig. 9.** Two-loop double scalar exchanging diagram

couplings associated with the first generation lepton. The early ansatz that the flavor-changing couplings are proportional to the square root of the products of related fermion masses may not be suitable for the lepton sector if the $\Delta a_\mu$ is found to be $> 50 \times 10^{-11}$. This indicates that both experimental and theoretical uncertainties need to be further reduced in order to explore the existence of new physics from $g-2$ of the muon. It has been shown that an alternative simple parameterization given in (16) is more attractive to understand the current experimental data. With such a parameterization, the decay rate of $\tau \to \mu\gamma$ is found to be close to the current experiment upper bound.

*Acknowledgements.* This work is supported in part by the Chinese Academy of Sciences and NSFC under Grant # 19625514. Y.F. Zhou acknowledges the support by the Alexander von Humboldt Foundation.

## Appendix

## A Two-loop double scalar diagrams in $g-2$ of the muon and $\mu \to e\gamma$

From the Yukawa interaction shown in (3), the $\bar{q}q\phi$ vertex has the following form in $d$ dimensions:

$$\mathrm{i}g\mu^{\epsilon/2}(Y_1 + Y_2\gamma_5), \tag{A.1}$$

where $\mu$ is the renormalization scale and $\epsilon/2 = 2 - d/2$.

The total amplitude can be written as the product of lower and upper parts as follows:

$$\Gamma_\mu = M \cdot I_\mu. \tag{A.2}$$

The amplitude $M$ for the upper loop is given by

$$\begin{aligned} M = &-g^2\mu^\epsilon \cdot 2N_C \int \frac{\mathrm{d}^d l}{(2\pi)^d} \\ &\times [(A_1 + A_2\gamma_5)(\not{l} + \not{q} + m_f)(B_1 + B_2\gamma_5)(\not{l} + m_f)] \\ &\times \frac{1}{(l+q)^2 - m_\tau^2}\frac{1}{l^2 - m_f^2} \end{aligned} \tag{A.3}$$

where $N_C$ and $m_f$ are the color number and mass of the fermion $f$. For a $t$ quark $f = t$ and $N_C = 3$. $A_{1,2}$ and $B_{1,2}$ are the couplings of the vertex $A$ and $B$.

The amplitude $I_\mu$ for the lower loop is given by

$$\begin{aligned} I_\mu = &-g^2\mu^\epsilon \bar{\ell}(p_2)(C_1 + C_2\gamma_5)(\not{p}_2 - \not{q} + m_\tau) \\ &\times \gamma_\mu(\not{p}_1 - \not{q} + m_\tau)(D_1 + D_2\gamma_5)\ell(p_1) \\ &\times \frac{1}{(q-p_2)^2 - m_\tau^2} \cdot \frac{1}{(q-p_1)^2 - m_\tau^2} \cdot \frac{1}{(q^2 - m_\phi^2)^2}, \end{aligned} \tag{A.4}$$

where $C_{1,2}$ and $D_{1,2}$ are the couplings for the vertex $C$ and $D$.

After integrating over the lower loop and isolating the poles from the Feynman integration, we obtain

$$\begin{aligned} \Gamma_\mu = &\frac{-8 \cdot 2N_C g^4 (A_1B_1 - A_2B_2) m_\tau m_\mu}{(4\pi)^4} \\ &\times \int_0^1 \mathrm{d}x 2x(1-x) \int_0^1 \mathrm{d}y \int_0^{1-y} \mathrm{d}z \\ &\times (y+z)(1-y-z) \\ &\times \Bigg( \Bigg( \left( \frac{2}{\epsilon} - 2\gamma_E + 2\ln 4\pi - \ln x(1-x) + \frac{1}{2} \right) \cdot f_{1,\mathrm{div}} \\ &+ 2 \cdot f_{1,\mathrm{con}} \Bigg) \\ &+ \frac{1}{2} C_{ab} R \cdot \Bigg( \left( \frac{2}{\epsilon} - 2\gamma_E + 2\ln 4\pi - \ln x(1-x) \right) \cdot f_{2,\mathrm{div}} \\ &+ 2 \cdot f_{2,\mathrm{con}} \Bigg) \Bigg) \\ &\times \bar{\ell}(C_1D_1 + C_2D_2 + (C_1D_2 + C_2D_1)\gamma_5) \frac{\mathrm{i}\sigma^{\mu\nu}k_\nu}{2m_\mu}\ell, \end{aligned} \tag{A.5}$$

with $\Delta' = (y+z)m_\tau^2 + (1-y-z)m_\phi^2$, $R = m_f^2/[x(1-x)]$ and $C_{ab} = 2A_2B_2/(A_1B_1 - A_2B_2)$.

In the large $m_f$ limit, i.e. $m_f^2 \gg (1/4)m_\phi^2 \gg m_\tau^2$, the functions $f_{1,\mathrm{div(con)}}$ and $f_{2,\mathrm{div(con)}}$ have the following forms:

$$\begin{aligned} f_{1,\mathrm{div}} &\to \frac{R}{\Delta'^2}, \quad f_{2,\mathrm{div}} \to -\frac{1}{\Delta'^2}, \\ f_{1,\mathrm{con}} &\to \frac{R}{2\Delta'^2}\left[1 - \ln\left(\frac{\Delta' R}{\mu^4}\right)\right], \\ f_{2,\mathrm{con}} &\to \frac{1}{2\Delta'^2}\left[1 + \ln\frac{\Delta' R}{\mu^4}\right]. \end{aligned} \tag{A.6}$$

After the renormalization in the $\overline{\mathrm{MS}}$ scheme for the upper loop, one finds

$$\begin{aligned} \Gamma_\mu = &\frac{-8 \cdot 2N_C g^4 m_\tau m_\mu (A_1B_1 - A_2B_2)}{(4\pi)^4} \\ &\times \int_0^1 \mathrm{d}x 2x(1-x) \int_0^1 \mathrm{d}y \int_0^{1-y} \mathrm{d}z \\ &\times (y+z)(1-y-z) \end{aligned}$$

$$\times \left[+\frac{3\Delta'+R}{\Delta'^2}\left(-\ln x(1-x)+\frac{1}{2}+\mathcal{F}(x)+\ln\frac{\Delta'}{\mu^2}\right)\right.$$
$$+2\cdot f_{1,\mathrm{con}}$$
$$-\frac{1}{\Delta'^2}\frac{1}{2}C_{ab}R\left(-\ln x(1-x)+\frac{1}{2}+\mathcal{F}(x)+\ln\frac{\Delta'}{\mu^2}\right)$$
$$\left.+\frac{1}{2}C_{ab}R\left(2\cdot f_{2,\mathrm{con}}-\frac{1}{2}\right)+\frac{3\Delta'-2R}{2\Delta'^2}\right]$$
$$\times\bar{\ell}(p_2)(C_1D_1+C_2D_2+(C_1D_2+C_2D_1)\gamma_5)$$
$$\times\frac{\mathrm{i}\sigma_{\mu\nu}k^\nu}{2m_\mu}\ell(p_1), \tag{A.7}$$

with

$$\mathcal{F}(x)=\ln\frac{m_f^2-x(1-x)m_\tau^2}{\mu^2}. \tag{A.8}$$

In the limit of $m_f^2\gg(1/4)m_\phi^2\gg m_\tau^2$, the above equation can be simplified to

$$\Gamma_\mu=-\frac{N_Cg^4m_\tau m_\mu m_f^2(A_1B_1+A_2B_2)}{16\pi^4m_\phi^4}\left(-\frac{5}{2}+\ln\frac{m_\phi^2}{m_\tau^2}\right)$$
$$\times\left((C_1D_1+C_2D_2)\bar{\ell}(p_2)\frac{\mathrm{i}\sigma_{\mu\nu}k^\nu}{2m_\mu}\ell(p_1)\right.$$
$$\left.+\ (C_1D_2+C_2D_1)\bar{\ell}(p_2)\frac{\mathrm{i}\sigma_{\mu\nu}k^\nu\gamma_5}{2m_\mu}\ell(p_1)\right). \tag{A.9}$$

Therefore its contribution to $g-2$ of the muon is as follows:

$$\Delta a_\mu=-\frac{N_Cg^4m_\tau m_\mu m_f^2}{16\pi^4m_\phi^4}\left(-\frac{5}{2}+\ln\frac{m_\phi^2}{m_\tau^2}\right)$$
$$\times(A_1B_1+A_2B_2)(C_1D_1+C_2D_2). \tag{A.10}$$

In the real coupling case, for scalar exchange, one has

$$gA_1=gB_1=Y_{ff},\quad gC_1=gD_1=Y_{\mu\tau}, \tag{A.11}$$

and the others are zero. Similarly for pseudo-scalar exchange the couplings are

$$gA_2=gB_2=\mathrm{i}Y_{ff},\quad gC_2=gD_2=\mathrm{i}Y_{\mu\tau}. \tag{A.12}$$

Therefore, the two-loop double scalar (pseudo-scalar) diagram's contribution to $\Delta a_\mu$ is

$$\Delta a_\mu=\mp\frac{N_Cm_\tau m_\mu m_f^2}{16\pi^4m_\phi^4}\left(-\frac{5}{2}+\ln\frac{m_\phi^2}{m_\tau^2}\right)Y_{ff}^2Y_{\mu\tau}^2. \tag{A.13}$$

For the decay $\mu\to e\gamma$, the effective vetex is

$$\Gamma_\mu^{(\mu\to e\gamma)}=-\frac{N_Cg^4m_\tau m_\mu m_f^2(A_1B_1+A_2B_2)}{16\pi^4m_\phi^4}$$
$$\times\left(-\frac{5}{2}+\ln\frac{m_\phi^2}{m_\tau^2}\right) \tag{A.14}$$
$$\times\left((C_1'D_1+C_2'D_2)\bar{\ell}(p_2)\frac{\mathrm{i}\sigma_{\mu\nu}k^\nu}{2m_\mu}\ell(p_1)\right.$$
$$\left.+\ (C_1'D_2+C_2'D_1)\bar{\ell}(p_2)\frac{\mathrm{i}\sigma_{\mu\nu}k^\nu\gamma_5}{2m_\mu}\ell(p_1)\right),$$

where $C_1'$ and $C_2'$ are the Yukawa couplings for the $\tau e\phi$ vertex. The decay rate is then given by

$$\Gamma(\mu\to e\gamma)=\frac{1}{16\pi m_\mu}\overline{\sum}\left|e\Gamma_\mu^{(\mu\to e\gamma)}\epsilon^\mu\right|^2. \tag{A.15}$$

## References


1. G.W. Bennett (Muon g-2 Collaboration) (2002), hep-ex/0208001
2. H.N. Brown et al. (Muon g-2 Collaboration), Phys. Rev. Lett. **86**, 2227 (2001), hep-ex/0102017
3. F. Jegerlehner, talk given at the Workshop Centre de Physique Theorique Marseille, France, 14–16 March 2002
4. K. Hagiwara, A.D. Martin, D. Nomura, T. Teubner, talk given by T. Teubner at ICHEP'02, Amsterdam, The Netherlands, 24–31 July 2002
5. See for example, U. Chattopadhyay, D.K. Ghosh, S. Roy, Phys. Rev. D **62**, 115001 (2000); L.L. Everett, G.L. Kane, S. Rigolin, L.T. Wang, Phys. Rev. Lett. **86**, 3484 (2001); J.L. Feng, K.T. Matchev, Phys. Rev. Lett. **86**, 3480 (2001); U. Chattopadhyay, P. Nath, Phys. Rev. Lett. **86**, 5854 (2001); S. Komine, T. Moroi, M. Yamaguchi, Phys. Lett. B **506**, 93 (2001); J. Hisano, K. Tobe, Phys. Lett. B **510**, 197 (2001); J.E. Kim, B. Kyae, H.M. Lee, Phys. Lett. B **520**, 298 (2001); S.P. Martin, J.D. Wells, Phys. Rev. D **64**, 035003 (2001); H. Baer, C. Balazs, J. Ferrandis, X. Tata, Phys. Rev. D **64**, 035004 (2001); G.C. McLaughlin, J.N. Ng, Phys. Lett. B **493**, 88 (2000); S.C. Park, H.S. Song, Phys. Lett. B **506**, 99 (2001); C. S. Kim, J.D. Kim, J. Song, Phys. Lett. B **511**, 251 (2001); K. Agashe, N.G. Deshpande, G.H. Wu, Phys. Lett. B **511**, 85 (2001); K. Choi, K. Hwang, S.K. Kang, K.Y. Lee, W.Y. Song, Phys. Rev. D **64**, 055001 (2001); E. Ma, M. Raidal, Phys. Rev. Lett. **87**, 011802 (2001); Erratum-ibid. **87**, 159901 (2001)]; R. Arnowitt, B. Dutta, B. Hu, Y. Santoso, Phys. Lett. B **505**, 177 (2001); V.D. Barger, T. Falk, T. Han, J. Jiang, T. Li, T. Plehn, Phys. Rev. D **64**, 056007 (2001); R. Casadio, A. Gruppuso, G. Venturi, Phys. Lett. B **495**, 378 (2000); C.H. Chen, C.Q. Geng, Phys. Lett. B **511**, 77 (2001); Z. z. Xing, Phys. Rev. D **64**, 017304 (2001)
6. Y.-L. Wu, Y.-F. Zhou, Phys. Rev. D **64**, 115018 (2001), hep-ph/0104056
7. M. Raidal, Phys. Lett. B **508**, 51 (2001), hep-ph/0103224
8. Y.L. Wu, L. Wolfenstein, Phys. Rev. Lett. **73**, 1762 (1994); L. Wolfenstein, Y.L. Wu, Phys. Rev. Lett. **73**, 2809 (1994). For more detailed analyses, see Y.L. Wu, Carnegie-Mellon Report, hep-ph/9404241, 1994 (unpublished); A Model for the Origin and Mechanisms of CP Violation, in Proceedings at 5th Conference on the Intersections of Particle and Nuclear Physics, St. Petersburg, FL, 31 May–6 June 1994, pp. 338, edited by S.J. Seestrom (AIP, New York 1995)
9. T.D. Lee, Phys. Rev. D **8**, 1226 (1973)
10. T.D. Lee, Phys. Rept. **9**, 143 (1974)
11. P. Sikivie, Phys. Lett. B **65**, 141 (1976); H.E. Haber, G.L. Kane, T. Sterling, Nucl. Phys. B **161**, 493 (1979); N.G. Deshpande, E. Ma, Phys. Rev. D **18**, 2574 (1978); H. Georgi, Hadronic J. **1**, 155 (1978); J.F. Donoghue, L.-F. Li,

Phys. Rev. D **19**, 945 (1979); A.B. Lahanas, C.E. Vayonakis, Phys. Rev. D **19**, 2158 (1979); L.F. Abbott, P. Sikivie, M.B. Wise, Phys. Rev. D **21**, 1393 (1980); G.C. Branco, A.J. Buras, J.M. Gerard, Nucl. Phys. B **259**, 306 (1985); B. McWilliams, L.-F. Li, Nucl. Phys. B **179**, 62 (1981); J.F. Gunion, H.E. Haber, Nucl. Phys. B **272**, 1 (1986); J. Liu, L. Wolfenstein, Nucl. Phys. B **289**, 1 (1987)
12. T.P. Cheng, M. Sher, Phys. Rev. D **35**, 3484 (1987)
13. M. Sher, Y. Yuan, Phys. Rev. D **44**, 1461 (1991)
14. A. Dedes, H.E. Haber (2001), hep-ph/0105014
15. A. Dedes, H.E. Haber, JHEP **05**, 006 (2001), hep-ph/0102297
16. M. Krawczyk (2001), hep-ph/0103223
17. J.R. Primack, H.R. Quinn, Phys. Rev. D **6**, 3171 (1972); W.A. Bardeen, R. Gastmans, B. Lautrup, Nucl. Phys. B **46**, 319 (1972); J.P. Leveille, Nucl. Phys. B **137**, 63 (1978); H.E. Haber, G.L. Kane, T. Sterling, Nucl. Phys. B **161**, 493 (1979); E.D. Carlson, S.L. Glashow, U. Sarid, Nucl. Phys. B **309**, 597 (1988)
18. J.D. Bjorken, S. Weinberg, Phys. Rev. Lett. **38**, 622 (1977); S.M. Barr, A. Zee, Phys. Rev. Lett. **65**, 21 (1990)
19. D. Chang, W.-F. Chang, C.-H. Chou, W.-Y. Keung, Phys. Rev. D **63**, 091301 (2001), hep-ph/0009292
20. K. Cheung, C.-H. Chou, O.C.W. Kong (2001), hep-ph/0103183
21. D. Atwood, L. Reina, A. Soni, Phys. Rev. Lett. **75**, 3800 (1995), hep-ph/9507416
22. D. Atwood, L. Reina, A. Soni, Phys. Rev. D **55**, 3156 (1997), hep-ph/9609279
23. Y.L. Wu, Y.F. Zhou, Phys. Rev. D **61**, 096001 (2000), hep-ph/9906313
24. M. Sher, Phys. Lett. B **487**, 151 (2000), hep-ph/0006159
25. S. Nie, M. Sher, Phys. Rev. D **58**, 097701 (1998), hep-ph/9805376
26. S.K. Kang, K.Y. Lee (2001), hep-ph/0103064
27. R. Diaz, R. Martinez, J.A. Rodriguez (2000), hep-ph/0010149
28. D.E. Groom et al. (Particle Data Group Collaboration), Eur. Phys. J. C **15**, 1 (2000)
29. D. Chang, W.S. Hou, W.Y. Keung, Phys. Rev. D **48**, 217 (1993), hep-ph/9302267
30. H. Fritzsch, Nucl. Phys. B **155**, 189 (1979)
31. H. Fritzsch, Phys. Lett. B **73**, 317 (1978)